Metal precipitation at grain boundaries in silicon: Dependence on grain boundary character and dislocation decoration

T. Buonassisi,[a] A. A. Istratov, and M. D. Pickett
Department of Materials Science and Engineering, University of California, Berkeley, California 94720 and Materials Science Division, Lawrence Berkeley National Laboratory, Berkeley, California 94720

M. A. Marcus
Advanced Light Source, Lawrence Berkeley National Laboratory, Berkeley, California 94720

T. F. Ciszek[b]
National Renewable Energy Laboratory, Golden, Colorado 80401

E. R. Weber
Department of Materials Science and Engineering, University of California, Berkeley, California 94720 and Materials Science Division, Lawrence Berkeley National Laboratory, Berkeley, California 94720

Synchrotron-based analytical microprobe techniques, electron backscatter diffraction, and defect etching are combined to determine the dependence of metal silicide precipitate formation on grain boundary character and microstructure in multicrystalline silicon (mc-Si). Metal silicide precipitate decoration is observed to increase with decreasing atomic coincidence within the grain boundary plane (increasing Σ values). A few low-Σ boundaries contain anomalously high metal precipitate concentrations, concomitant with heavy dislocation decoration. These results provide direct experimental evidence that the degree of interaction between metals and structural defects in mc-Si can vary as a function of microstructure, with implications for mc-Si device performance and processing. © 2006 American Institute of Physics. [DOI: 10.1063/1.2234570]

Currently, over half of all solar cells produced worldwide are made from multicrystalline silicon (mc-Si). While these devices have comparatively lower efficiencies than those made of higher-purity, single crystalline silicon (sc-Si), the lower manufacturing costs result in a more favorable *cost per watt peak* ($/W_p$), the financial figure of merit for mainstream photovoltaic (PV) technologies. To heighten this advantage, considerable efforts are being invested into improving the efficiencies of mc-Si materials.

Transition metal impurities, which are found in concentrations as high as $10^{14}-10^{16}$ cm^{-3} in most mc-Si materials,[1–3] play a large role in decreasing mc-Si device performance relative to sc-Si. In mc-Si materials, grain boundaries are now understood to be the locations where metals are found in the highest concentrations,[4,5] aside from isolated inclusions. Because of high local impurity concentrations and limited impurity solubility and diffusivity at gettering temperatures,[6,7] precipitate dissolution may be incomplete during solar cell processing. Thus, on the time scale of solar cell device processing, these reservoirs may act as virtually "inexhaustible" sources for metal atoms within the bulk, with the potential to contaminate neighboring intragranular regions.[8] It is clear then that understanding the precipitation behavior of metals at different types of grain boundaries is of fundamental technological importance for mc-Si technology. Surprisingly, despite over 50 years of intensive effort dedicated to understanding solute-grain boundary interactions in polycrystalline ceramics and metals [including impurity precipitation,[9–11] oxidation,[12] (liquid metal)

embrittlement and fracture,[13,14] fatigue,[15] and numerous other phenomena[16,17]], far fewer literature reports describe solute-grain boundary interactions in silicon with due attention to grain boundary microstructure,[18–22] and fewer still systematically compare the interactions of impurities with different *types* of grain boundaries, mostly via indirect electrical measurements.[23–26] In this study, we directly measure the local metal silicide precipitate concentrations at various types of grain boundaries, identifying clear trends of preferential precipitate formation at certain types of boundaries.

Multicrystalline float zone[27] (mc-FZ) was selected for this study because it can be grown with very high densities of various types of grain boundaries. At 1200 °C in a quartz tube furnace, a controlled amount of copper and nickel impurities was introduced into mc-FZ, which was then quenched to room temperature in silicone oil, and then reannealed at 655 °C for 2.5 h. With a fairly uniform average grain size below a square millimeter, this anneal provided sufficient time for copper and nickel to diffuse to and form metal silicide precipitates at the most energetically favorable sites. After chemically etching to remove the surface silicide layer, synchrotron-based analytical microprobe techniques[28] were used to directly measure the amount of metals accumulated in metal silicide precipitates at individual grain boundaries in the material. X-ray fluorescence microscopy (μ-XRF) was performed at Beamline 10.3.2 (Ref. 29) of the Advanced Light Source at Lawrence Berkeley National Laboratory (LBNL) to map metal impurity distributions. While μ-XRF has a modest bulk sensitivity of $\sim 10^{16}$ cm^{-3} metal atoms,[30] its microfocused beam makes it a powerful tool for detecting metal-rich precipitates several tens or hundreds of nanometers in size,[28] wherein local metal concentrations reach several tens of percent. The concentrations of

---

[a] Also at Applied Science and Technology Group; present address: Evergreen Solar, Inc.; electronic mail: buonassisi@alumni.nd.edu
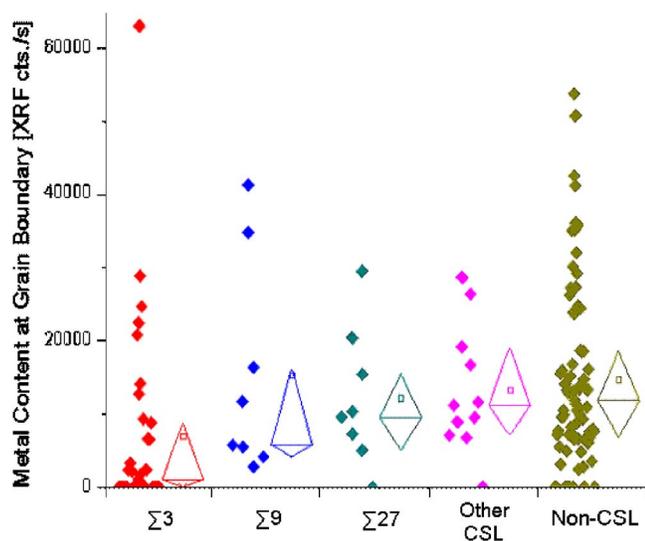[b] Present address: Siliconsultant, P.O. Box 1453, Evergreen, CO 80437.

FIG. 1. (Color online) The dependence of metal precipitate concentration (measured by μ-XRF) on grain boundary character (EBSD) for 141 grain boundaries identified in a mc-Si sample. In general, metal precipitate decoration tends to increase with decreasing degree of atomic coincidence in the grain boundary plane (increasing Σ value). The metal-precipitate-decorated low-Σ boundaries are further discussed in Fig. 2. To the right of each data cluster, the open diamonds represent the 25th and 75th percentiles and the median. The open box is the mean.
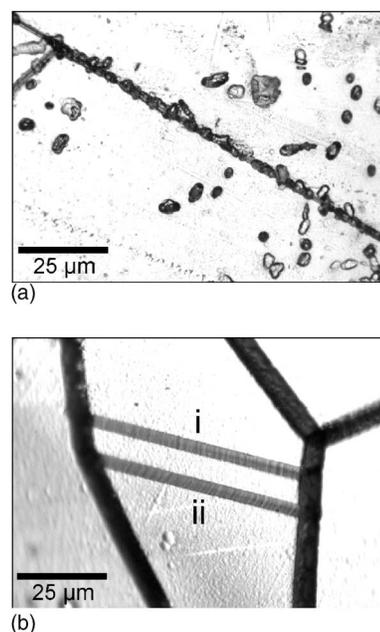

FIG. 2. Optical micrographs of defect-etched $\Sigma 3$ boundaries. (a) Those in the top 25th percentile of $\Sigma 3$ boundaries in Fig. 1 (heavily decorated by metal precipitates) contain high densities of dislocations. (b) Those in the lower 75th percentile (lightly or negligibly decorated by metal precipitates) contain fewer or no dislocation etch pits, as exemplified by the parallel $\Sigma 3$ boundaries denoted "i" and "ii."

precipitated metals at 141 grain boundaries were compared by integrating μ-XRF counts from background-subtracted line scans across individual grain boundaries. To determine the character of each grain boundary, electron backscatter diffraction[31] (EBSD) measurements were performed on the same samples, using an FEI Strata 235 scanning electron microscope at the National Center for Electron Microscopy (NCEM) at LBNL. For grain boundary characterization, the allowable angular deviation was set according to the standard Brandon criterion $[\Delta\theta \leqslant 15° \Sigma^{-1/2}$ (Ref. 32)].

From the data (summarized in Fig. 1), it is observed that boundaries with low coincidence site lattice (CSL) indices (Σ values) generally contain lower concentrations of precipitated metals than boundaries with high CSL indices or non-CSL boundaries. The data generally suggest that metal precipitation increases with increasing Σ value, consistent with the trends reported for CSL boundary electrical activity by Ihlal *et al.*[23] and Chen *et al.*[25,26] The likely physical explanation for this is that the high degree of atomic coincidence and low level of bond distortion found in low-Σ boundaries may offer a lower density of energetically favorable sites for impurity atoms to segregate and precipitate. For the same reasons, it may also be possible that impurity diffusion is slower along lower-Σ boundaries, potentially retarding precipitate nucleation and growth. Consistent with these explanations, larger concentrations of precipitated metals tend to be found at nonstraight, random-angle boundaries, depicted by the higher data points in the "non-CSL" category in Fig. 1.

Upon closer inspection of the data, it is observed that a minority of grain boundaries with low Σ values also contains surprisingly high concentrations of precipitated metals. Consider, for instance, the upper 25th percentile of data points in Fig. 1, indicating anomalously high metal contents at some $\Sigma 3$ boundaries. To identify the cause of this variability, a defect etch (Sopori etch[33]) was used to reveal dislocations. It was found that $\Sigma 3$ boundaries decorated with metal precipi-

tates are also heavily decorated by dislocations, as shown in Fig. 2(a).

Conversely, the majority of $\Sigma 3$ grain boundaries with lesser or negligible concentrations of precipitated metals contains either no dislocations [e.g., Fig. 2(b)] or many fewer dislocations. These observations are consistent with literature reports of increased electrical activity at boundaries with piled-up dislocations.[34–36] A high density of dislocations may be required to bring a sufficient number (perhaps tens or hundreds) of metal atoms sufficiently close together to overcome the nucleation barrier. Dislocations are also known to provide efficient diffusion pathways for impurities, by so-called pipe diffusion.

In conclusion, μ-XRF was used to directly measure the metal content at various types of mc-Si grain boundaries, the characters of which were determined by EBSD. These experimental results directly confirm that metal precipitation tends to vary inversely with the degree of atomic coincidence in the grain boundary plane, consistent with previous results measuring grain boundary electrical activity. Upon occasion, a high concentration of metal silicide precipitates is also observed at grain boundaries with low Σ values exhibiting a high degree of dislocation decoration. The identification of the largest reservoirs for metals in mc-Si may serve to guide efforts to "grain boundary engineer" mc-Si materials that have weaker internal sinks for metals, and hence, improved gettering responses and electrical performances.

[1] D. Macdonald, A. Cuevas, A. Kinomura, Y. Nakano, and L. J. Geerligs, J. Appl. Phys. **97**, 033523 (2005).

[2] D. Macdonald, A. Cuevas, A. Kinomura, and Y. Nakano, *Proceedings of the 29th IEEE Photovoltaic Specialists Conference, New Orleans, 19–24 May 2002* (IEEE, New York, 2002), p. 1707.

[3] A. A. Istratov, T. Buonassisi, R. J. McDonald, A. R. Smith, R. Schindler, J. A. Rand, J. P. Kalejs, and E. R. Weber, J. Appl. Phys. **94**, 6552 (2003).

[4] T. Buonassisi, A. A. Istratov, M. Heuer, M. Marcus, R. Jonczyk, J. Isenberg, B. Lai, Z. Cai, S. Heald, W. Warta, R. Schindler, G. Willeke, and E. R. Weber, J. Appl. Phys. **97**, 074901 (2005).

[5] T. Buonassisi, A. A. Istratov, M. D. Pickett, M. Heuer, J. P. Kalejs, G. Hahn, M. A. Marcus, B. Lai, Z. Cai, S. M. Heald, T. F. Ciszek, R. F. Clark, D. W. Cunningham, A. M. Gabor, R. Jonczyk, S. Narayanan, E. Sauar, and E. R. Weber, Prog. Photovoltaics (in press).

[6] P. S. Plekhanov, R. Gafiteanu, U. M. Gosele, and T. Y. Tan, J. Appl. Phys. **86**, 2453 (1999).

[7] M. Seibt, A. Sattler, C. Rudolf, O. Voß, V. Kveder, and W. Schröter, Phys. Status Solidi A **203**, 696 (2006).

[8] T. Buonassisi, A. A. Istratov, S. Peters, C. Ballif, Z. Cai, B. Lai, R. Schindler, G. Willeke, and E. R. Weber, Appl. Phys. Lett. **87**, 121918 (2005).

[9] P. L. Ryder and W. Pitsch, Acta Metall. **14**, 1437 (1966).

[10] S. Watanabe, Y. Takamatsu, N. Sakaguchi, and H. Takahashi, J. Nucl. Mater. **283–287**, 152 (2000).

[11] U. Dahmen, S. Hagège, F. Faudot, T. Radetic, and E. Johnson, Philos. Mag. **84**, 2651 (2004).

[12] S. Yamura, Y. Igariashi, S. Tsurekawa, and T. Watanabe, Acta Mater. **47**, 1163 (1999).

[13] T. Watanabe and S. Tsurekawa, Acta Mater. **47**, 4171 (1999).

[14] C. L. Briant, Mater. Sci. Technol. **17**, 1317 (2001).

[15] Y. Gao, M. Kumar, R. K. Nalla, and R. O. Ritchie, Metall. Mater. Trans. A **36A**, 3325 (2005).

[16] *Grain boundaries: Their character, Characterisation and Influence on Properties*, edited by I. R. Harris and I. P. Jones (IOM, London, 2001).

[17] G. Palumbo and K. T. Aust, Can. Metall. Q. **34**, 165 (1995).

[18] M. J. Kim, R. W. Carpenter, Y. L. Chen, and G. H. Schwuttke, Ultramicroscopy **40**, 258 (1991).

[19] X. Portier, A. Ihlal, and R. Rizk, Phys. Status Solidi A **161**, 75 (1997).

[20] J.-L. Maurice and C. Colliex, Appl. Phys. Lett. **55**, 241 (1989).

[21] A. Ihlal and R. Rizk, J. Phys. D **29**, 3096 (1996).

[22] M. F. Chisholm, A. Maiti, S. J. Pennycook, and S. T. Pantelides, Phys. Rev. Lett. **81**, 132 (1998).

[23] A. Ihlal, R. Rizk, and O. B. M. Hardouin Duparc, J. Appl. Phys. **80**, 2665 (1996).

[24] J. Lu, M. Wagener, G. Rozgonyi, J. Rand, and R. Jonczyk, J. Appl. Phys. **94**, 140 (2003).

[25] J. Chen, T. Sekiguchi, D. Yang, F. Yin, K. Kido, and S. Tsurekawa, J. Appl. Phys. **96**, 5490 (2004).

[26] J. Chen, D. Yang, X. Zhenqiang, and T. Sekiguchi, J. Appl. Phys. **97**, 033701 (2005).

[27] T. F. Ciszek and T. H. Wang, J. Cryst. Growth **237–239**, 1685 (2002).

[28] T. Buonassisi, A. A. Istratov, M. A. Marcus, M. Heuer, M. D. Pickett, B. Lai, Z. Cai, S. M. Heald, and E. R. Weber, Solid State Phenom. **108–109**, 577 (2005).

[29] M. A. Marcus, A. A. MacDowell, R. Celestre, E. Domning, K. Franck, A. Manceau, G. Morrison, T. Miller, H. A. Padmore, and R. E. Sublett, J. Synchrotron Radiat. **11**, 239 (2004).

[30] S. A. McHugo, A. C. Thompson, C. Flink, E. R. Weber, G. Lamble, B. Gunion, A. MacDowell, R. Celestre, H. A. Padmore, and Z. Hussain, J. Cryst. Growth **210**, 395 (2000).

[31] F. J. Humphreys, J. Mater. Sci. **36**, 3833 (2001).

[32] D. G. Brandon, Acta Metall. **14**, 1479 (1966).

[33] B. L. Sopori, Appl. Opt. **27**, 4676 (1988).

[34] K. Yang, G. H. Schwuttke, and T. F. Ciszek, J. Cryst. Growth **50**, 301 (1980).

[35] W. Seifert, G. Morgenstern, and M. Kittler, Semicond. Sci. Technol. **8**, 1687 (1993).

[36] J. Chen, T. Sekiguchi, R. Xie, P. Ahmet, T. Chikyo, D. Yang, S. Ito, and F. Yin, Scr. Mater. **52**, 1211 (2005).